2021 International Conference on Intelligent Technologies (CONIT)
Karnataka, India. June 25-27, 2021

Wireless Energy Harvesting Cognitive Radio Network under Finite-Capacity Battery for Nakagami-m Fading

Nayanika Biswas
Electronics and Communication Engineering Dept.
Delhi Technological University
New Delhi, India
nayanikabiswas_2k17ec109.dtu.ac.in

Piyush Tewari*
Electronics and Communication Engineering Dept.
Delhi Technological University
New Delhi, India
piyushtewari@dtu.ac.in

***Abstract*—We present a radio frequency(RF) based energy harvesting(EH) cognitive radio network(CRN) with finite-capacity battery at the secondary source(SS). All channels in the network undergo Nakagami-m fading. The secondary network's(SN) performance is analysed using outage probability and throughput. To obtain a simplified analytical model, we derive the expressions for the upper bound of the outage probability and the lower bound for the throughput of the SN. The analytical expressions for the PDF and CDF of harvested energy of the SN are also derived. The impact of finite battery constraint on the performance of the SN is investigated and analytical expressions for outage probability and throughput are derived. Results show that for an optimal battery capacity, the performance of the SN is identical to that of the infinite-capacity battery assisted CRN. The paper also presents a method to obtain the optimal battery capacity of the CRN under Nakagami-m fading. All analytical results are verified against Monte-Carlo simulations in MATLAB.**

***Index Terms*—Cognitive Radio, Wireless Energy Harvesting, Finite-Capacity Battery Model, Nakagami-m Fading Channel**

I. Introduction

With the rise of Internet of Things(IOT), there is an increase in the use of wireless devices used by individuals. A huge amount of spectrum is required to support all these wireless devices. Spectrum is a natural resource licensed by Governments. Businesses have opted for digitisation and shifted from brick and mortar setups. However, this natural resource is scarce and under utilized. Spectrum Holes are frequency bands in a spectrum over whose entirety the secondary user can transmit signal without causing interference at the primary receiver. Cognitive Radios are being introduced to tackle this shortage and under utilisation of spectrum by taking advantage of these spectrum holes [7]. Cognitive radios Networks(CRNs) allow opportunist spectrum sharing and spectrum sensing systems called Secondary Users(SUs)(also known as unlicensed users) that dynamically adapt to unused spectrums allocated to licensed users called Primary Users(PU) by adapting its parameters in real-time. [7]- [6]. The performance and design of CRNs for relay-assisted and non-relay assisted networks have been investigated in the scientific literature [1], [4].

Another major concern is that with the rise in wireless devices, there is an increase in their power requirement. To prolong the lifetime of energy-constrained wireless networks, make them self-sustainable, and promote green communication, energy harvesting techniques that harness energy from sources like heat, wind, light and radio-waves are being studied [14], [12]. Recently, EH due to ambient radio frequency(RF) signals has caught the attention of the research community as it provides energy self sufficiency conveniently to a low powered communication system [11], [8], [2]. With increase demand and technological advances in low power devices in academia and industry, wireless energy harvested[WEH] from RF signals will be practically realisable, specially for wireless sensor network(WSN) nodes. [8], [15].

Commonly used EH secondary receiving(SR) architecture are power splitting(PS) architecture and time splitting(TS) architecture [14]. In PS, the received signal power is split into two fractions, one for EH and the other for information retrieval [14], [8]. Whereas, in TS the energy harvesting-information transmitting(EH-IT) cycle is split into two fractions, one for EH and information retrieval by the receiver node and other for IT [8], [15].

In [13], an underlay non relay assisted secondary network(SN) is analyzed using outage probability and the results show that the energy harvested by the SN from the PU transmitter's RF signals is sufficient for information transmission of SN as well as relaying information for the PN. In [5], the outage probability and throughput of an underlay relay assisted CRN with TS protocol is analysed. [5] uses Rayleigh fading channel model and multiple PU transmitters and receivers.In [10], an non-relay underlay EH CRN is proposed and the impact of multiple energy- constrained receivers in SN is studied. Most works on CRNs that provide a good understanding of the subject assume channels to undergo Rayleigh fading [13], [5]. They also assume infinite storage capacity at the energy harvesting nodes of the SN [13], [5]. While Rayleigh fading channels simplify analytical solutions, but they represent limited practical scenarios [3]. Similarly, the rechargeable battery at the WEH node of the SN has a finite battery capacity. Nakagami-m fading channels represent a variety of scenarios whose severity can be tuned using

978-1-7281-8583-5/21/$31.00 ©2021 IEEE

the shape parameter. Further, for m = 1, m $<$ 1, and m $>$ 1, a Nakagami-m fading channel can be modelled as a Rayleigh fading channel, Hoyt fading channel, and Rice fading channel respectively [3]. In [3], the outage probability of dual-hop cognitive amplify-and-forward (AF) relay-assisted CRN undergoing Nakagami-m fading is studied. It assumes a finite maximum transmit power at SN, provides comparison between two proposed transmit power constraints and shows that the irrespective of the transmit power constraint, the diversity order is strictly defined by the minimum fading severity between the two transmitting nodes at the SN. In [9], an overlay CRN is considered which nakagami-m fading channels, in which a secondary transmitter (ST) relays the information of a PU transmitter toward a PU receiver.

A. Motivation and Contribution

We noted a lack of analytical models in the technical literature for WEH-CRN under HU architecture, which studies the optimal battery capacity required at the SN, under Nakagami-m fading condition, for optimal performance. In order to study the impact of finite battery constraint on the performance of WEH-CRN along with other system parameters, the following contributions are made by the proposed work:

1) We derive analytical expressions for the upper bound of the outage probability as well as the lower bound for the throughput for the SN for a non-relay-assisted WEH underlay CRN with finite-capacity battery at SS and investigate its impact on the performance of SN under decode and forward protocol for delay-sensitive networks. The following constraints are enforced: 1) The harvested energy is limited by the maximum storage capacity of the rechargeable battery at SS; 2) The maximum transmit power at SS is limited by the energy harvested; 3) The maximum transmit power at SS is limited by the peak interference power threshold set by PU; 4) The interference power from multiple PU transmitters at SD limits reliable communication between SS and SD.
2) Novel expressions for the PDF and CDF for the harvested energy at the EH node with finite-capacity storage(i.e., SS) are derived.
3) The outage probability and throughput for SN are evaluated for different battery storage capacity values, and the optimum battery capacity is identified.
4) We show that the impact of residual harvested energy remaining in the battery on the performance of the SN is minimal.

II. Network Model

We consider a non-relay underlay CRN where an energy constrained SS uses the PU's licensed spectrum to transmit to the SD. The PN has N primary transmitters and M primary receivers. All PU transmitters are assumed to be clustered about a point due to their proximity. Similarly, all PU receivers too are clustered about a central point as they are closely located [5]. The SS only uses radio frequency signals from the PU transmitters to harvest energy. The harvested energy is stored in a finite capacity battery which can be modelled as a rechargeable super-capacitor with a switching circuit to alternate between the energy harvesting and signal transmission cycles of the CRN. As shown in figure 1, the coefficients $g_{S,i}$ for $i = 1, 2, ..., M$, represent the channel gains from the ith PU_{RX} to SS respectively. The coefficient h denotes the channel gain coefficient from SS to SD. Similarly, the coefficients $f_{S,j}$, $f_{D,j}$ for $j = 1, 2, , .., N$, represent the channel gains from the jth PU_{TX} to SS and SD respectively. All channels are modelled assuming the distance between the jth PU_{TX} and SS, and SD as $d_{S,j}$, $d_{D,j}$, respectively. The distance between ith PUrx and SS is denoted as $d_{S,i}$ respectively. And the distance between SS and SD are denoted as d4, respectively. The link gain realizations $|h|^2, |g_S|^2, |f_{S,j}|^2, |f_{D,j}|^2$ are gamma distributed with shape parameters $m_h, m_{g_{S,i}}, m_{f_{S,j}}, m_{f_{D,j}}$, and $\beta_h, \beta_{g_{S,i}}$, $\beta_{f_{S,j}}$, and $\beta_{f_{D,j}}$ respectively. $\beta_{f_{S,j}} = {d_{1,j}}^{-n}$, n being the path loss factor. $f_{S,j}$ $\forall j$ that link the PU transmitters and the SS are assumed to be identically distributed. Similarly, $f_{D,j}$ $\forall j$ that link PU transmitters and SD follow identical distribution. Moreover, identical distribution is assumed for the link gain from SS to PU receivers due to close proximity of all the transmitters and all the receivers about their respective central points. However, $f_{S,j}$, $f_{D,j}$, and $g_{S,i}$ are non-identically distributed wrt each other. The energy harvesting and information transmission is

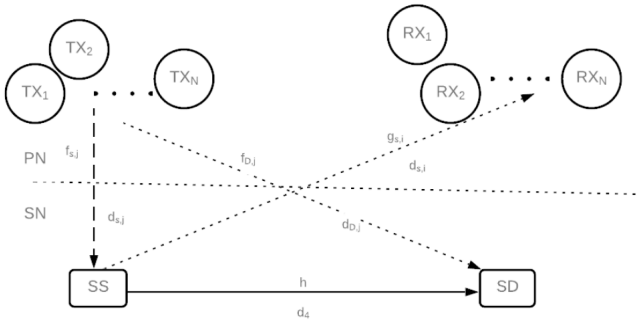

Fig. 1. System Model for WEH CRN. The SS has finite-capacity battery.

performed in alternate cycles, following time splitting architecture. T is the total time period for one cycle and α is the ratio at which every cycle is split into two sub cycles, one for harvesting energy from the PU transmitters and other for information transmission(IT).

The energy harvested at the SS under infinite battery capacity is

$$E_{hsi} = \eta\alpha \mathrm{P}_{\mathrm{PU_{tx}}} \sum_{j=1}^{N} |f_{1,j}|^2 \mathrm{T} \tag{1}$$

where η represents the energy conversion coefficient, $P_{PU_{tx}}$ denotes transmitted power from all PU transmitters and $|f_{1,j}|$ is Nakagami-m distributed with the PDF

$$f(x) = \frac{2m^m x^{2m-1} e^{\frac{-mx^2}{\beta_{1,j}}}}{\Gamma(m)\beta_{1,j}^m} \tag{2}$$

where $\beta_{1,j} = E[X^2]$ and $\Omega = \frac{\beta_{1,j}}{m}$ The link gain realisation $|f_{1,j}|^2$ follows gamma distribution whose PDF and CDF are defined as

$$f(x) = \frac{x^{m-1} e^{\frac{-x}{\Omega}}}{\Omega^m \Gamma(m)} \tag{3}$$

$$F(x) = \frac{\gamma(m, \frac{x}{\Omega})}{\Gamma(m)} \tag{4}$$

where $\gamma(m,x) = \int_0^x t^{x-1} e^{-t} dt$ is the lower incomplete gamma function.

Due to the finite-battery constraint the energy harvested at the SS is

$$E_{hs} = \min(E_{hsi}, B_{max}) \tag{5}$$

where B_{max} is the maximum battery capacity energy at SS.

The transmit power at SS is

$$P_s = \min\left(\frac{E_{hs}}{(1-\alpha)T}, \frac{P_I}{\min\{|g_{1,i}|^2\}}\right) \tag{6}$$

where P_I is the maximum permissible interference power at PU_{rx} due to SS. In a transmission cycle, when the term $\frac{E_{hs}}{(1-\alpha)T}$ is larger than the term $\frac{P_I}{\min\{|g_{1,i}|^2\}}$, the maximum transmitted energy is limited by the latter term thus giving rise to residual energy. This residual energy remaining in the battery is considered to be negligible for obtaining the upper bound on the outage probability of the SN. To avoid interference at PU receivers due to high power transmitted by the SS, the peak interference constraint is imposed such that it does not exceed P_I.

The signal to interference ratio (SIR) at SS is defined as

$$\Gamma_S = \min\left(\frac{E_{hs}}{(1-\alpha)T}, \frac{P_I}{Y}\right)\frac{X}{Z_2} \tag{7}$$

$Z_1 = P_{PU_{tx}} \sum_{j=1}^{N} |f_{S,j}|^2, Z_2 = P_{PU_{tx}} \sum_{j=1}^{N} |f_{D,j}|^2, X = |h|^2, Y = \min\{|g_{S,i}|^2\}$

We evaluate the performance of the SN using two system performance metrics, outage probability and network throughput.

Outage Probability(OP) is defined as the probability that the SIR at SS is below a threshold value γ_{th} [5]. We consider the presented non-relay assisted underlay network to be in outage iff outage is suffered by the SS-SD link. Its expression is given by

$$P_{out}(\gamma_{th}) = 1 - Pr\{\Gamma_S \leq \gamma_{th}\} \tag{8}$$

where Γ_S is the SIR at the SD. Throughput of a network is stated as the amount of data received at the receiver end after transmission through the communication link[9]. We evaluate the throughput in delay-sensitive mode. In this mode, the SS transmits information at a fixed rate R_{ds} to SD. The throughput in this mode is given as[14]

$$\tau_{ds} = (1-\alpha) R_{ds} (1 - P_{out}(\gamma_{th})) \tag{9}$$

where τ_{ds} is the rate of successful transmissions during the transmission cycle, given that the SIR is more than the threshold γ_{th} at SD.

III. Performance Analysis

We evaluate the performance of the network based on certain thresholds above which the network is considered reliable. In this section, we derive the analytical solution for the upper bound for OP of the proposed CRN model.

The OP can also be written as

$$P_{out}(\gamma_{th}) = \mathrm{I}_1 + \mathrm{I}_2 - \mathrm{I}_3 \tag{10}$$

where $I_1 = P(V < \zeta), I_2 = P(\frac{P_I}{Y} < \zeta), I_3 = P(V < \zeta, \frac{P_I}{Y} < \zeta), \zeta = \frac{\gamma_{th} Z_2}{X}$ and $V = \frac{E_{hs}}{(1-\alpha)T}$

The PDF and CDF of the E_{hs} is required to derive the mathematical expression of the upper bound for outage probability using eq. (8). We obtain the CDF and PDF of E_{hsi} as,

$$F_{E_{hsi}} = \frac{\Gamma\{\sum_{j=1}^{N} m_{S,j}, \frac{x}{c\Omega}\}}{\Gamma\{\sum_{j=1}^{N} m_{S,j}\}} \tag{11}$$

$$f_{E_{hsi}} = gamma\left(\sum_{j=1}^{N} m_{S,j}, c\Omega\right) \tag{12}$$

where $\Gamma(.,x)$ is the upper incomplete gamma function, and $gamma(.,.)$ denotes the gamma distribution and $c = \eta P_{PU_{TX}} T$. As seen in eq (5), the energy stored in the battery is equal to E_{hsi} when it is less than B_{max}, else it is equal to B_{max}, as B_{max} acts as the ceiling for the maximum harvested energy that can be stored in the battery. Thus the CDF can be written as

$$Pr(E_{hs} < ehs | ehs < B_{max}) = Pr(E_{hsi} < ehs)$$

and

$$Pr(E_{hs} < ehs | ehs > B_{max} = 1 \text{as} Pr(E_{hs} < B_{max}) = 1 \tag{13}$$

The PDF can be derived by piece-wise differentiation of the CDF. Using eq (13), the CDF of E_{hs} can be expressed as

$$F_{E_{hs}}(ehs) = \frac{\Gamma\{\sum_{j=1}^{N} m_{S,j}, \frac{x}{c\Omega}\}}{\Gamma\{\sum_{j=1}^{N} m_{S,j}\}} [u(ehs) - u(ehs - B_{max})] + u(ehs - B_{max}) \tag{14}$$

Thus the optimal B_{max} value required to achieve performance of SN that is identical to that of infinite-capacity battery assisted CRN can be obtained using the following relation

$$F_{E_{hs}}(B_{max}) = \frac{\Gamma\{\sum_{j=1}^{N} m_{S,j}, \frac{B_{max}}{c\Omega}\}}{\Gamma\{\sum_{j=1}^{N} m_{S,j}\}} = 0.99 \tag{15}$$

$$B_{max} = \gamma^{-1}\left(\sum_{j=1}^{N} m_{S,j}, 0.99\Gamma\{\sum_{j=1}^{N} m_{S,j}\}\right)(c\Omega) \tag{16}$$

where $\gamma^{-1}(.,.)$ denotes the inverse of lower incomplete gamma function. Using definitions given by eq. (10), we solve for I_1,

$$\begin{aligned}
I_1 &= Pr\{min(B_{max}, kZ_1) < \zeta(1-\alpha)T\} \\
&= Pr\{X < \frac{\gamma_{th} Z_2 (1-\alpha)T}{B_{max}}\} \times Pr\{Z_1 > \frac{B_{max}}{k}\} \\
&+ Pr\{X < \frac{\gamma_{th} Z_2 (1-\alpha)T}{kZ_1} \cap Z_1 < \frac{B_{max}}{k}\} \\
&= \left[\frac{1}{C_1} \times \left(\frac{C_2^{m_h}\Gamma(m_h + M_{jD})}{m_h (C_2 + \frac{1}{\Omega'_{jD}})^{M_{jD}+m_h}}\right)\right. \\
&\left. \times F_{21}\left(1, m_h + M_{jD}; m_h + 1; \frac{C_2}{C_2 + \frac{1}{O'_{jD}}}\right)\right] \\
&\times \left(1 - \frac{\gamma\left(M_{jS}, \frac{B_{max}}{k\Omega'_{jS}}\right)}{\Gamma(M_{jS})}\right) \\
&+ \int_0^{\frac{B_{max}}{k}} \left[\frac{1}{C_4}\left(\frac{C_3^{m_h}\Gamma(m_h + M_{jD})}{m_h (C_3 + \frac{1}{\Omega'_{jD}})^{M_{jD}+m_h}}\right)\right. \\
&\times F_{21}\left(1, m_h + M_{jD}; m_h + 1; \frac{C_3}{C_3 + \frac{1}{O'_{jD}}}\right) \\
&\left. \times e^{\frac{-z_1}{\Omega'_{jS}}} z_1^{M_{jS}-1} dz_1\right]
\end{aligned} \tag{17}$$

where $k = \eta\alpha T$, $C_1 = \Gamma(m_h)\Gamma(M_{jD})\left(\Omega'_{jD}\right)^{M_{jD}}$,
$C_2 = \frac{\gamma_{th}(1-\alpha)T}{B_{max}\Omega_h}, C_3 = \frac{\gamma_{th}(1-\alpha)T}{Z_1 k \Omega_h}$,
$C_4 = C_1\Gamma(M_{jS})\left(\Omega'_{jS}\right)^{M_{jS}}$,

and $F_{21}\left(a, b; c; z\right)$ is a hypergeometric function.

Solving for I2,

$$\begin{aligned}
I_2 &= Pr\{\frac{P_I}{Y} < \zeta\} \\
&= Pr\{X < \frac{\gamma_{th} Z_2 Y}{P_I}\} \\
&= F_{Z_2 Y}\left[\frac{\gamma\left(m_h, \frac{\gamma_{th} Z_2 Y}{P_I \Omega_h}\right)}{\Gamma(m_h)}\right] \\
&= \int_0^{\infty} \left[\frac{1}{C_6} \times \left(\frac{C_5^{m_h}\Gamma(m_h + M_{jD})}{m_h (C_5 + \frac{1}{\Omega'_{jD}})^{M_{jD}+m_h}}\right)\right. \\
&\times F_{21}\left(1, m_h + M_{jD}; m_h + 1; \frac{C_5}{C_5 + \frac{1}{O'_{jD}}}\right) \\
&\left. \times \frac{\gamma\left(m_{iS}, \frac{y}{\Omega i S}\right)^{M-1}}{\Gamma(m_{iS})^{M-1}} \times e^{\frac{-y}{\Omega'_{iS}}} y^{m_{iS}-1} dy\right]
\end{aligned} \tag{18}$$

where $C_5 = \frac{\gamma_{th} Y}{P_I \Omega_h}, C_6 = \frac{C_1\Gamma(m_{iS})(\Omega_{iS})^{M_{iS}}}{M}$

Solving for I_3,

$$\begin{aligned}
I_3 &= P(V < \zeta, \frac{P_I}{Y} < \zeta), \\
&= \int_{z_2=0}^{\infty}\int_{x=0}^{\infty} I_{31} I_{32} f_{Z_2}(z_2) f_X(x) dz_2 d_x
\end{aligned} \tag{19}$$

as I_{31} and I_{32} are independent of each other wrt x and z_2. From eq (13)-(14), I_{31} can be simplified as

$$\begin{aligned}
I_{31} &= Pr\{E_{hsi} < ehs | ehs < B_{max}\} \\
&+ Pr\{E_{hsi} < ehs | ehs > B_{max}\} \\
&\text{`} = F_{E_{hsi}}(ehs)\left[u(ehs) - u(ehs - B_{max})\right] \\
&+ 1 \times u(ehs - B_{max}) \\
&= \frac{\gamma\left(M_{jS}, \frac{\gamma_{th} Z_2 (1-\alpha T}{X C_7 \Omega'_{jS}}\right)}{\Gamma(M_{jS})}\left[u(ehs) - u(ehs - B_{max})\right] \\
&+ 1 \times u(ehs - B_{max})
\end{aligned} \tag{20}$$

$ehs = \frac{\gamma_{th} Z_2 (1-\alpha)T}{X}, C_7 = \frac{\eta\alpha}{(1-\alpha)}$,

$$I_{32} = Pr\{Y > \frac{P_I X}{\gamma_{th} Z_2}\} = 1 - \left[\frac{\gamma\left(m_{iS}, \frac{P_I X}{\gamma_{th} Z_2 \Omega_{iS}}\right)}{\Gamma(m_{iS})}\right]^M \tag{21}$$

Using eq. (21) and (20) in (19), we write I_3 for $Z_2 < \frac{B_m axx}{\gamma_{th}(1-\alpha T}$

$$\begin{aligned}
I_3 &= \int_{x=0}^{\infty}\int_{z_2=0}^{\frac{xB_{max}}{\gamma_{th}(1-\alpha T}} \left(1 - \left[\frac{\gamma\left(m_{iS}, \frac{P_I X}{\gamma_{th} Z_2 \Omega_{iS}}\right)}{\Gamma(m_{iS})}\right]^M\right) \\
&\times \frac{\gamma\left(M_{jS}, \frac{\gamma_{th} Z_2 (1-\alpha T}{X C_7 \Omega'_{jS}}\right)}{\Gamma(M_{jS})} \\
&\times \frac{z_2^{M_{jD}-1} e^{\frac{-z_2}{\Omega'_{jD}}}}{\Gamma(M_{jD})(\Omega_{jD})'^{M_{jD}}} \frac{x^{m_h-1} e^{\frac{-x}{\Omega_h}}}{\Gamma(m_h)(\Omega_h)^{m_h}} \times dz_2 dx
\end{aligned} \tag{22}$$

and for $z_2 > \frac{B_{max} x}{\gamma_{th}(1-\alpha T}$

$$\begin{aligned}
I_3 &= \int_{x=0}^{\infty}\int_{z_2=0}^{\frac{xB_{max}}{\gamma_{th}(1-\alpha T}} \left(1 - \left[\frac{\gamma\left(m_{iS}, \frac{P_I X}{\gamma_{th} Z_2 \Omega_{iS}}\right)}{\Gamma(m_{iS})}\right]^M\right) \\
&\times \frac{z_2^{M_{jD}-1} e^{\frac{-z_2}{\Omega'_{jD}}}}{\Gamma(M_{jD})(\Omega_{jD})'^{M_{jD}}} \frac{x^{m_h-1} e^{\frac{-x}{\Omega_h}}}{\Gamma(m_h)(\Omega_h)^{m_h}} \times dx dz_2
\end{aligned} \tag{23}$$

IV. Results

In this section we analyse the performance of the SN of the proposed WEH-CRN model and discuss the implications of finite-capacity battery and other system parameters on it. The results of the analytical model for outage probability and throughput for the SN are presented and verified with Monte-Carlo simulations. Excellent agreement between the results of the simulations and analytical expressions is obtained.

The PU transmitters are clustered about (0,1) without loss of generality and the PU receivers are clustered around (1,1). SS and SD are positioned at (0,0) and (1,0) respectively. The

system parameters, until unless specifically mentioned, are assumed as $N = M = 3$, $\alpha = 0.5, \eta = 0.8$, and $T = 1$ [5]. The shape parameters, until unless specifically mentioned, are assumed to be $m_h = 2, m_{g_{S,i}} = 2, m_{f_{S,j}} = 3, m_{f_{D,j}} = 3$.

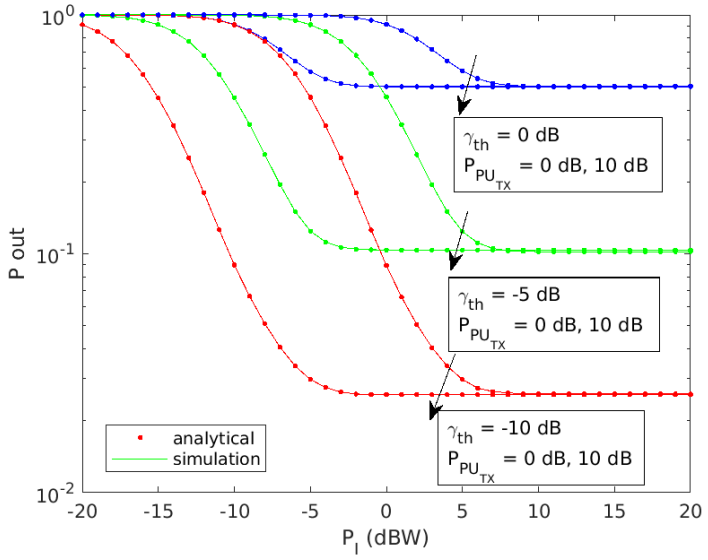

Fig. 2. OP(P_{out}) as a function of P_I for different $P_{PU_{TX}}$ and γ_{th}

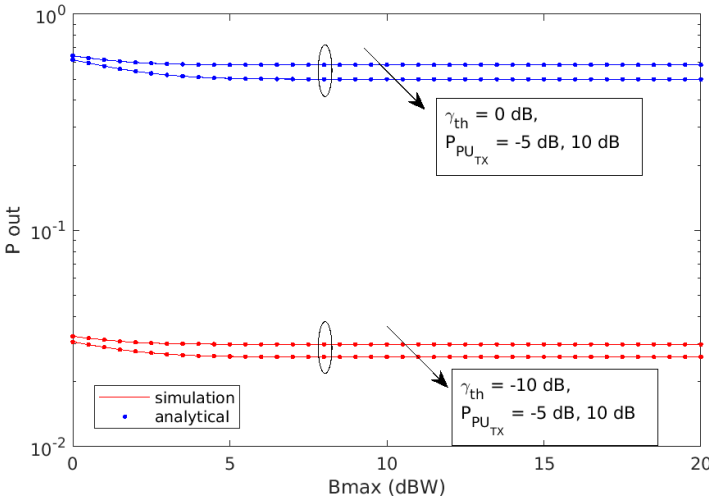

Fig. 3. OP(P_{out}) as a function of B_{max} for $P_{PU_{TX}} = 0dB$ and different γ_{th} and P_I

Fig 2 and 3 present the outage probability as a function of P_I and B_{max} respectively. We can see that the the OP decreases and ultimately saturates to a minimum as the P_I increases. This is because, as the permissible interference power increases beyond a value, the OP majorly depends on the harvested energy at the SS and becomes independent of P_I. Further, it can be observed that as the SIR threshold γ_{th} decreases, the OP decreases because of the relaxed constraint at SD for the successful detection of the transmitted signal. We can also see from the Fig 2 that for a larger $P_{PU_{tx}}$, the OP saturated for a higher P_I. This can be explained as the transmission power $P_{PU_{tx}}$ increases, the energy harvested at the SS increases, provided that the B_{max} is large enough, thus improving the SIR at the SD. We can see from Fig 3 that as the battery capacity increases the OP decreases and saturates to a minimum value where the OP becomes independent of the battery capacity. For a given γ_{th}, P_I and $P_{PU_{tx}}$, the system performance improves as B_{max} increases because it relaxes the constraint on maximum storage capacity of the finite battery at SS which in turn improves the SIR at the SD. It is also evident from Fig 3 that the system performance saturates to its minimum value after the optimal value of B_{max} at which it behaves identical to the asymptotic case for which the battery capacity is assumed to be infinite. The performance of SN after this optimal B_{max} value is independent of the battery capacity and depends on other system parameters like α and $P_{PU_{tx}}$. As seen in fig 3, the optimal B_{max} is observed to be 5.011 units. This agrees perfectly with the optimal B_{max} obtained from the eq (16), thus proving the validity of the eq (14).

Fig 4 illustrates the outage probability as a function of $P_{PU_{tx}}$. Here the OP increases with increase in $P_{PU_{tx}}$ for a fixed P_I until it reaches to unity and saturates. This is because increase in E_{hs} due to large $P_{PU_{tx}}$ is overpowered by the increase in interference at the SD. As the SIR is limited by P_I constraint, the OP eventually becomes independent of $P_{PU_{tx}}$.The result also shows that for a given γ_{th}, as the interference constraint relaxes, the OP saturates for a higher value of $P_{PU_{tx}}$. This is because increased tolerance to interference at the PU receivers allows storage of more harvested energy, given that B_{max} is large enough. The fig 4 also confirms the behaviour of OP wrt γ_{th}, i.e. OP increases with the increase in γ_{th}.

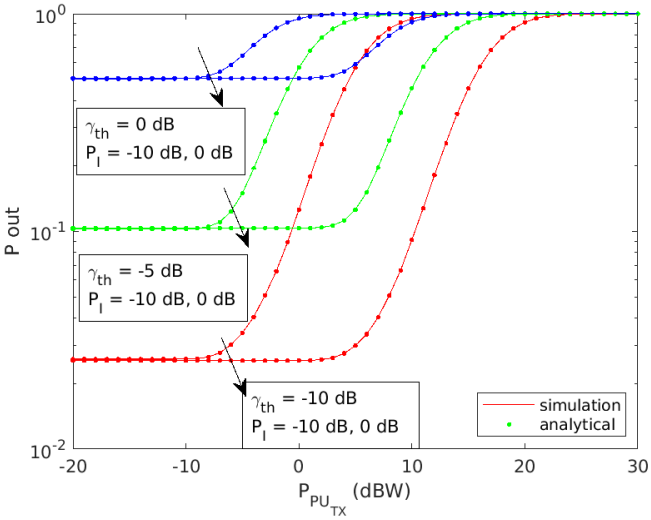

Fig. 4. OP(P_{out}) as a function of $P_{PU_{TX}} = 0dB$ for different γ_{th} and P_I

Fig 5 shows the delay-sensitive throughput of the SN as a function of P_I. For a fixed $P_{PU_{tx}}$, throughput increases and saturates at a maximum value as P_I increases. This is because

as the tolerance to interference at the PU receivers increases, the SS can transmit at higher power during the transmission cycle. For a higher value of $P_{PU_{tx}}$, the throughput increases and reaches its maximum value for a larger value of P_I. This is evident from the right shift in the throughput curve for $P_{PU_{tx}} = 10dB$.

Fig 6 shows that the OP for the proposed model is in close agreement with the OP curve which considers the effect of residual energy. This result proves that the proposed HU architecture based model provides a tight upper bound for the OP of the SN. Thus for a mathematically tractable solution, we can neglect the impact of residual energy.

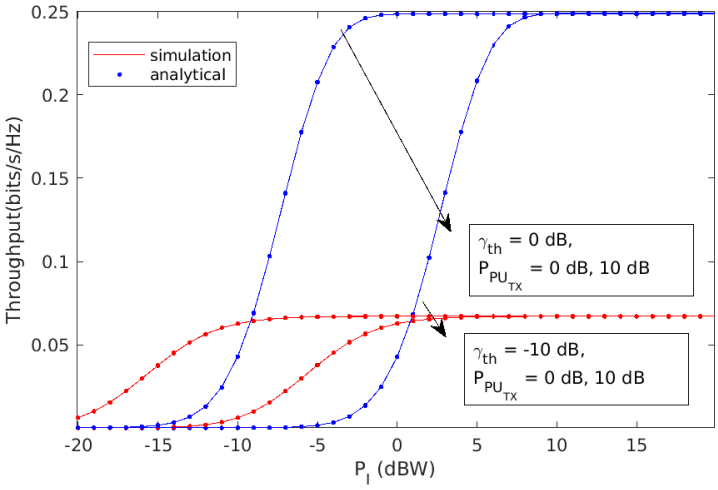

Fig. 5. Throughput as a function of P_I for different $P_{PU_{TX}}$ and γ_{th}

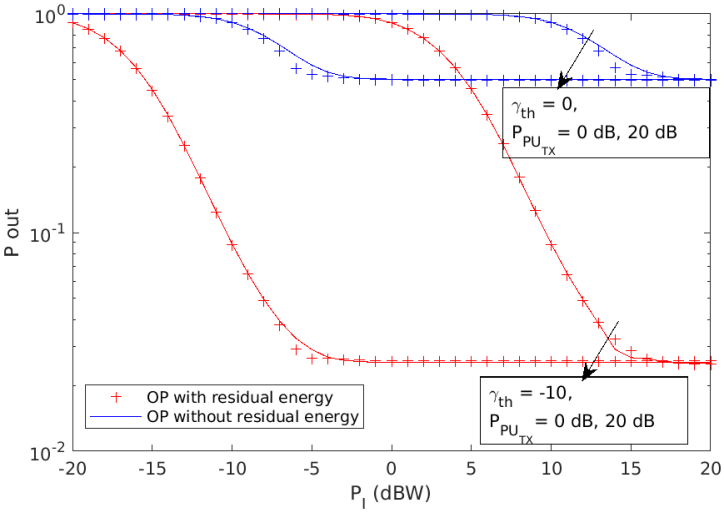

Fig. 6. Comparison Between the OP for WEH CRN considering residual energy in the battery with the proposed model

V. Conclusion

In this work, we presented the performance analysis for a WEH underlay non-relay CRN under HU protocol for Nakagami-m fading channels in terms of outage probability and throughput. The analytical expression for the upper bound of outage probability was obtained. We proposed novel PDF and CDF expressions for harvested energy at the SS to derive the expressions for outage probability and throughput. Our results show that optimal performance for the SN can be obtained with a finite-capacity battery, and in this region, the bound is in excellent agreement with the model considering the effects of residual energy remaining in the battery. We also presented a method to identify the optimum battery size corresponding to the optimal performance at the SN. Close agreement between the analytical and simulation results proves the validity of the proposed model.

References

[1] Mohamed M Abdallah, Ahmed H Salem, Mohamed-Slim Alouini, and Khalid A Qaraqe. Adaptive discrete rate and power transmission for spectrum sharing systems. *IEEE transactions on wireless communications*, 11(4):1283–1289, 2012.

[2] Hayder Al-Hraishawi and Gayan Amarasuriya Aruma Baduge. Wireless energy harvesting in cognitive massive mimo systems with underlay spectrum sharing. *IEEE Wireless Communications Letters*, 6(1):134–137, 2016.

[3] T. Q. Duong, D. B. da Costa, M. Elkashlan, and V. N. Q. Bao. Cognitive amplify-and-forward relay networks over nakagami- m fading. *IEEE Transactions on Vehicular Technology*, 61(5):2368–2374, 2012.

[4] YuanYuan He and Subhrakanti Dey. Throughput maximization in cognitive radio under peak interference constraints with limited feedback. *IEEE transactions on vehicular technology*, 61(3):1287–1305, 2012.

[5] Y. Liu, S. A. Mousavifar, Y. Deng, C. Leung, and M. Elkashlan. Wireless energy harvesting in a cognitive relay network. *IEEE Transactions on Wireless Communications*, 15(4):2498–2508, 2016.

[6] Yi Liu, Yan Zhang, Rong Yu, and Shengli Xie. Integrated energy and spectrum harvesting for 5g wireless communications. *IEEE Network*, 29(3):75–81, 2015.

[7] J. Mitola and G. Q. Maguire. Cognitive radio: making software radios more personal. *IEEE Personal Communications*, 6(4):13–18, 1999.

[8] Ali A Nasir, Xiangyun Zhou, Salman Durrani, and Rodney A Kennedy. Relaying protocols for wireless energy harvesting and information processing. *IEEE Transactions on Wireless Communications*, 12(7):3622–3636, 2013.

[9] B. V. Nguyen, H. Jung, D. Har, and K. Kim. Performance analysis of a cognitive radio network with an energy harvesting secondary transmitter under nakagami- m fading. *IEEE Access*, 6:4135–4144, 2018.

[10] L. Sibomana, H. Zepernick, and H. Tran. Wireless information and power transfer in an underlay cognitive radio network. In *2014 8th International Conference on Signal Processing and Communication Systems (ICSPCS)*, pages 1–7, 2014.

[11] Arooj Mubashara Siddiqui, Leila Musavian, Sonia Aissa, and Qiang Ni. Performance analysis of relaying systems with fixed and energy harvesting batteries. *IEEE Transactions on Communications*, 66(4):1386–1398, 2017.

[12] Kaya Tutuncuoglu and Aylin Yener. Optimum transmission policies for battery limited energy harvesting nodes. *IEEE Transactions on Wireless Communications*, 11(3):1180–1189, 2012.

[13] Zihao Wang, Zhiyong Chen, Ling Luo, Zixia Hu, Bin Xia, and Hui Liu. Outage analysis of cognitive relay networks with energy harvesting and information transfer. In *2014 IEEE international conference on communications (ICC)*, pages 4348–4353. IEEE, 2014.

[14] Fangchao Yuan, Shi Jin, Kai-Kit Wong, QT Zhang, and Hongbo Zhu. Optimal harvest-use-store design for delay-constrained energy harvesting wireless communications. *Journal of Communications and Networks*, 18(6):902–912, 2016.

[15] Rui Zhang and Chin Keong Ho. Mimo broadcasting for simultaneous wireless information and power transfer. *IEEE Transactions on Wireless Communications*, 12(5):1989–2001, 2013.